

PAPER

Novel Woods–Saxon stochastic resonance system for weak signal detection^{*}

To cite this article: Yong-Hui Zhou *et al* 2020 *Chinese Phys. B* **29** 040503

View the [article online](#) for updates and enhancements.

You may also like

- [Stochastic resonance induced performance enhancement of MEMS cantilever biosensors](#)
Priyanka Singh and R D S Yadava
- [Enhancement of bionic cilia flow rate sensor signals by single-well stochastic resonance](#)
Yihang Fu, Xinwei Zhang, Leyang Lv et al.
- [Stochastic resonance in Hindmarsh-Rose neural model driven by multiplicative and additive Gaussian noise](#)
Lianbing Xu, Gang Zhang, Lujie Bi et al.

Novel Woods–Saxon stochastic resonance system for weak signal detection*

Yong-Hui Zhou(周永辉), Xue-Mei Xu(许雪梅)[†], Lin-Zi Yin(尹林子),
Yi-Peng Ding(丁一鹏), Jia-Feng Ding(丁家峰), and Ke-Hui Sun(孙克辉)

School of Physics and Electronics, Central South University, Changsha 410083, China

(Received 18 July 2019; revised manuscript received 31 December 2019; accepted manuscript online 13 February 2020)

We propose a joint exponential function and Woods–Saxon stochastic resonance (EWSSR) model. Because change of a single parameter in the classical stochastic resonance model may cause a great change in the shape of the potential function, it is difficult to obtain the optimal output signal-to-noise ratio by adjusting one parameter. In the novel system, the influence of different parameters on the shape of the potential function has its own emphasis, making it easier for us to adjust the shape of the potential function. The system can obtain different widths of the potential well or barrier height by adjusting one of these parameters, so that the system can match different types of input signals adaptively. By adjusting the system parameters, the potential function model can be transformed between the bistable model and the monostable model. The potential function of EWSSR has richer shapes and geometric characteristics. The effects of parameters, such as the height of the barrier and the width of the potential well, on SNR are studied, and a set of relatively optimal parameters are determined. Moreover, the EWSSR model is compared with other classical stochastic resonance models. Numerical experiments show that the proposed EWSSR model has higher SNR and better noise immunity than other classical stochastic resonance models. Simultaneously, the EWSSR model is applied to the detection of actual bearing fault signals, and the detection effect is also superior to other models.

Keywords: stochastic resonance, weak signal detection, a joint exponential function and Woods–Saxon stochastic resonance, signal-to-noise ratio

PACS: 05.40.–a, 02.50.–r, 05.45.–a, 43.60.Hj

DOI: 10.1088/1674-1056/ab75ca

1. Introduction

Eliminating noise interference has become the key to weak signal detection owing to the problem that weak signals are often submerged in strong background noise. Compared to the traditional detection methods of noise suppression,^[1–9] researchers found another detection method. The theory of stochastic resonance (SR) was first proposed by Benzi and Nicolis *et al.*, when they conducted research on the ancient meteorological glaciers.^[10] SR is different from the general methods of weak signal detection. Instead of suppressing noise, it couples noise with the signal to enhance signal transmission performance, which means that the noise is beneficial for the detection of weak signals in SR systems. We can use the energy of noise to achieve the purpose of enhancing weak signals. Since SR has unique advantages in detecting weak signals in the background of strong noise, the theory was proposed, it has received great attention from scholars at home and abroad.^[11–16]

As an effective weak signal detection method, SR has been studied by many scholars around the world. For example, Asdi *et al.* studied the use of adaptive SR to detect weak signals in 1995.^[17] In 1998, Galdi *et al.* studied the use of SR to detect weak signals under additive white Gaus-

sian noise.^[18] Lutz applied SR for nonlinear signal detection in 2001.^[19] On the basis of in-depth study of the mechanism of SR, Leng *et al.* proposed re-scaling SR to solve the small parameter problem.^[20] Jin studied the Stochastic resonance in an under-damped bistable system driven by harmonic mixing signal in 2018.^[21] In the same year, Wang and Wang applied the adaptive stochastic resonance system to the terahertz radar signal detection.^[22] Subsequently, Xu *et al.* have made some progress in the random non-smooth system.^[23] Also, there are many researchers to obtain advances in SR.^[24–29] In addition, the researchers also proposed many new SR models such as the Woods–Saxon model.^[30–32]

However, for most domestic and foreign research on SR, the classic bistable SR model based on four-time reflection symmetry potential is mostly studied. In this system, the change of single parameter may cause a great change in the shape of the potential function, so it is difficult to obtain the optimal output signal-to-noise ratio by adjusting the system parameters, and the detection effect is still not satisfactory. Therefore, it is necessary to find new SR models to further enhance the performance of the output SNR. Based on previous studies, a new stochastic resonance (EWSSR) model is proposed based on the exponential function and the Woods–Saxon potential function to improve the output signal-to-noise

*Project supported by the National Natural Science Foundation of China (Grant No. 61501525) and the National Natural Science Foundation of Hunan Province of China (Grant No. 2018JJ3680).

[†]Corresponding author. E-mail: xuxuemei999@126.com

© 2020 Chinese Physical Society and IOP Publishing Ltd

<http://iopscience.iop.org/cpb> <http://cpb.iphy.ac.cn>

ratio and detection performance of the SR system. Compared with the classical SR model, the EWSSR model has three distinct merits: (1) The EWSSR model has more parameters and the system is more complicated, so the dynamic characteristics are richer. (2) The EWSSR potential can be designed accurately due to the system which can obtain different widths of the potential well or barrier height by adjusting one of these parameters, so the EWSSR can match to different types of input signals adaptively. (3) The proposed EWSSR model has higher SNR and better noise immunity than other classical SR models.

The rest of the paper is organized as follows: Section 2 introduces the principle of Woods–Saxon stochastic resonance (WS), presents a new model of joint exponential function, and analyzes the effect of system parameters on the output signal-to-noise ratio. In Section 3, we confirm that EWSSR is better than the traditional SR models by comparing the new model with other existing SR models in the aspects of SNR and the detection effect in time-frequency domain. In Section 4, the EWSSR system is applied to detect the fault characteristics of the outer rings of the bearing. The final section is devoted to the conclusion.

2. The EWSSR model

2.1. The Woods–Saxon potential function model

The WS well is nonlinear symmetric, which can be illustrated as follows:

$$U_{WS}(x) = -\frac{v_0}{1 + \exp[(|x| - r)/c]}, \quad (1)$$

where v_0 is used to change the depth of the well, r is used to determine the width of the well, and c is the steepness of the wall. The potential function of the WS potential well is shown in Fig. 1. We set the parameters $v_0 = 2$ and $r = 1$, and c varies from 0.01 to 0.25. It can be seen from Fig. 1 that the potential well is a square well when $c = 0$, and as c increases, the wall slope of the WS potential well becomes more and more gently.

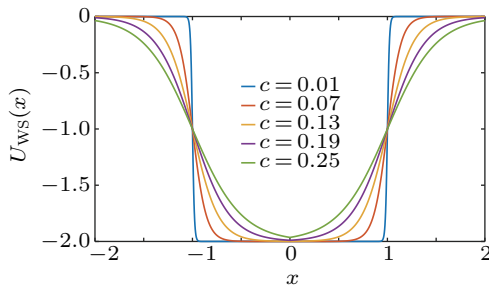


Fig. 1. WS potential function.

2.2. Exponential function model

The exponential function model is

$$U_e(x) = \frac{a}{b} \cdot \exp(|bx|), \quad (2)$$

where a and b are the system parameters. The potential function has no barrier, only one well, which is shown in Fig. 2. The width and depth of the well are adjusted by changing the values of a and b .

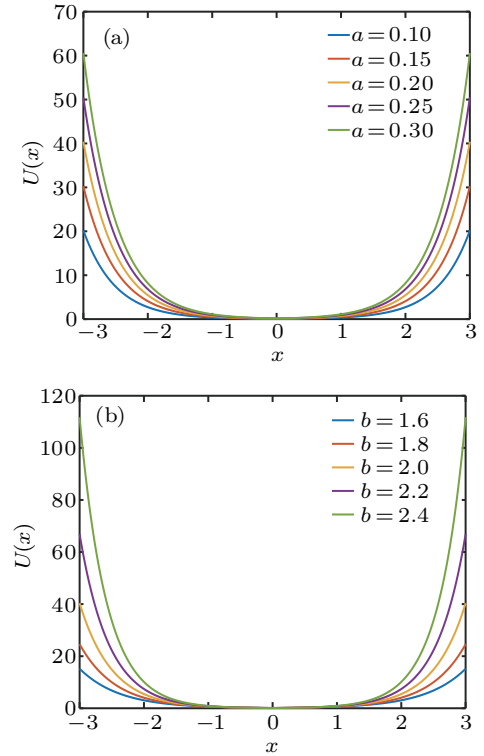


Fig. 2. Exponential function model. (a) Different system parameter a and fixed parameters with $b = 2.0$. (b) Different system parameter b and fixed parameters with $a = 0.20$.

2.3. Characteristics of the EWSSR model

Combining the exponential function and the Woods–Saxon potential function model, we put forward a new bistable potential well model, which is named as the EWSSR double potential well model. The potential function is expressed as

$$U(x) = U_e(x) - U_{WS}(x) = \frac{a}{b} \exp(|bx|) + \frac{v_0}{1 + \exp(\frac{|x| - r}{c})}. \quad (3)$$

It can be seen from Eq. (3) that the potential function has five system parameters: a , b , v_0 , c , r . They determine the shape of the potential function together. By adjusting the system parameters, the potential function model can be transformed between the bistable model and the monostable model. Therefore, the potential function model proposed in this paper contains the advantages of the traditional single potential well and double potential well models. Moreover, the influence of different parameters on the shape of the potential function has its own emphasis, making it easier for us to adjust the shape of the potential function, which can enable the system adaptively match with different input signals to generate an SR phenomenon. Thereby the system can be applied to detect different signals. The potential function of the EWSSR model is shown in Fig. 3. The system parameter is $a = 0.25$, $b = 1.5$,

$c = 0.25$, $v_0 = 5$, $r = 0.8$. By transforming the original single-well model and the WS model into the double-well model of EWSSR, particles would transition back and forth between the two potential wells, instead of oscillating within a single WS well. Therefore, the utilization of noise is improved and the output signal-to-noise ratio is enhanced.

Moreover, it can be seen from Figs. 4(a)–4(e) that the changes of different parameters have different influences on the shape of the potential function. Here a and b play a crucial role in the slope of the potential wall. As a or b increases, the slope of the potential well will be greater at the same time. With the increasing v , the barrier height will increase simultaneously. Because c decides the slope of the barrier, if the value of c becomes larger, the barrier will become smoother. Since r

decides the width of the well, if r becomes larger, the potential well will become wider too. Therefore, by adjusting the parameters, the dynamic characteristics of the system could be more abundant.

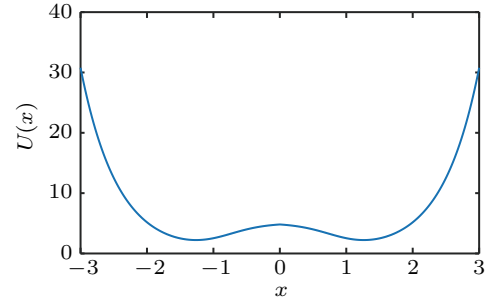


Fig. 3. EWSSR potential function.

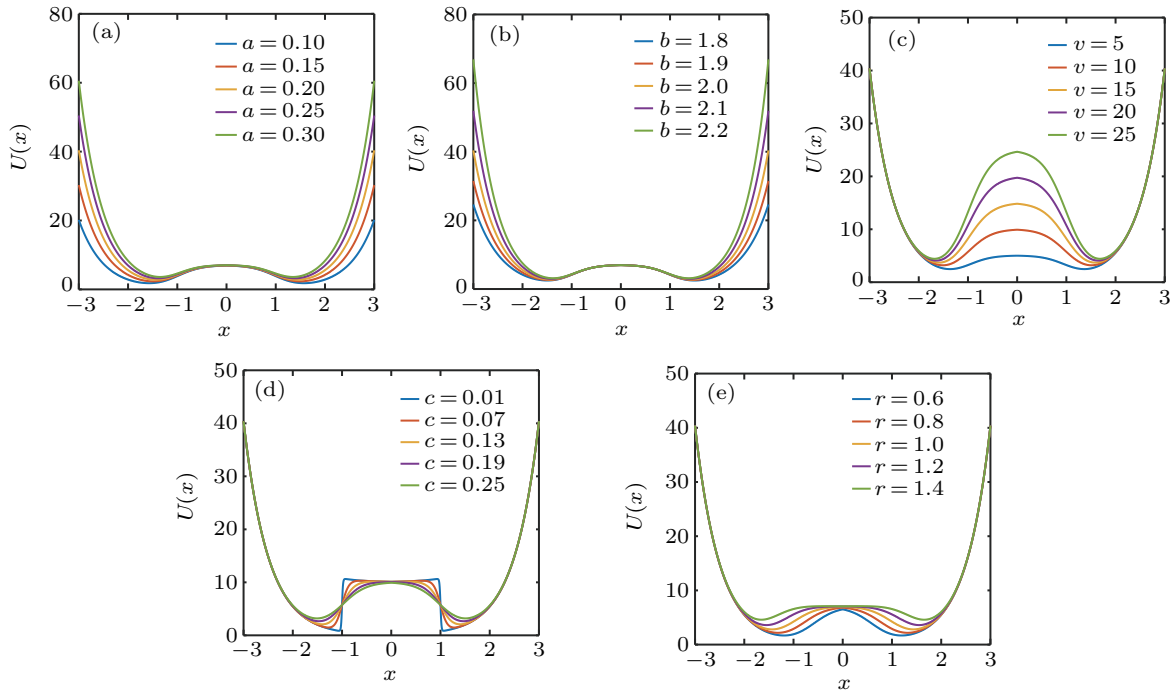


Fig. 4. The effect of varieties in individual parameter on the EWSSR potential function for (a) different system parameter a , (b) different b , (c) different v_0 , (d) different c , and (e) different r .

Compared with the EWSSR model in Fig. 4, it can be seen from Figs. 5 and 6 that in the SR and TSR models, when a single parameter changes, the shape of the potential function changes significantly, and the potential well and the barrier simultaneously change. This indicates that the parameters of the SR and TSR models are more difficult to adjust.

The SR system equation is obtained as follows:

$$\frac{dx}{dt} = -U'(x) + s(t) + n(t), \quad (4)$$

where $x(t)$ denotes the output signal, $s(t)$ denotes the input signal, $U(x)$ is the potential function, and $n(t) = \sqrt{2D}\xi(t)$ represents the Gaussian white noise with $E[n(t)n(t+\tau)] = 2D\delta(t)$, where D is the noise intensity and $\xi(t)$ is the Gaussian white noise with the mean of zero and the variance of unit.

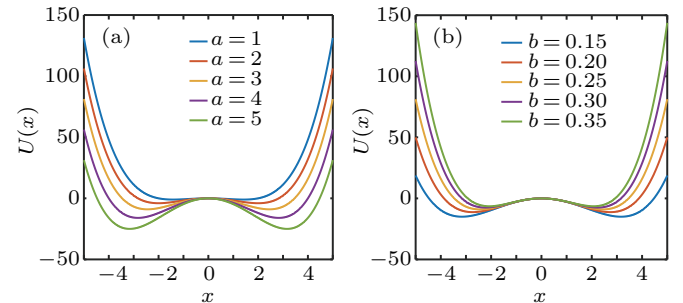


Fig. 5. The effect of varieties in individual parameter on the SR potential function for (a) different a and (b) for different b .

For the EWSSR potential function model, substituting Eq. (3) into Eq. (4), we can obtain the system equation of the EWSSR model as follows:

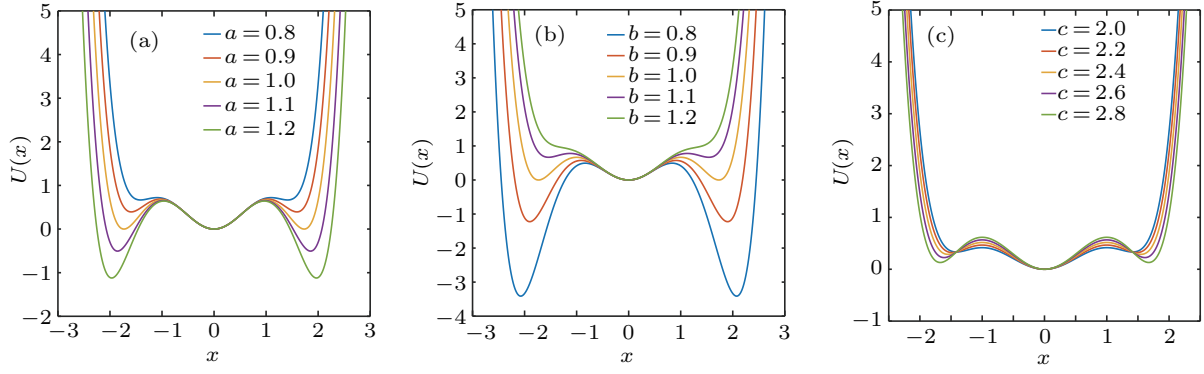


Fig. 6. The effect of varieties in individual parameter on the EWSSR potential function for (a) different a , (b) different b , and (c) different c .

$$\begin{aligned} \frac{dx}{dt} = & -a \exp(|bx|) \operatorname{sgn}(bx) + \frac{v_0}{c} \operatorname{sgn}(x) \\ & \times \exp\left(\frac{|x| - r}{c}\right) \left(1 + \exp\left(\frac{|x| - r}{c}\right)\right)^{-2} \\ & + s(t) + n(t), \end{aligned} \quad (5)$$

where $\operatorname{sgn}(x)$ is a symbol function. Its expression is

$$\operatorname{sgn}(x) = \begin{cases} 1, & x > 0, \\ 0, & x = 0, \\ -1, & x < 0. \end{cases} \quad (6)$$

2.4. Numerical implementation of EWSSR

Equation (5) is a first-order differential equation, which can be discretized using the fourth-order Runge–Kutta algorithm. The solution is as follows:

$$\begin{aligned} x' &= f(t, x), \quad x(t[0]) = x[0], \\ k_1 &= -ab \exp(|bx(i)|) \operatorname{sgn}(bx(i)) \\ &+ \frac{v_0}{c} \operatorname{sgn}(x(i)) \exp\left(\frac{|x(i)| - r}{c}\right) \\ &\times \left(1 + \exp\left(\frac{|x(i)| - r}{c}\right)\right)^{-\alpha-1} + s(i) + n(i), \\ k_2 &= -ab \exp\left(\left|b\left(x(i) + \frac{hk_1}{2}\right)\right|\right) \operatorname{sgn}\left(b\left(x(i) + \frac{hk_1}{2}\right)\right) \\ &+ \frac{v_0}{c} \operatorname{sgn}\left(x(i) + \frac{hk_1}{2}\right) \exp\left(\frac{|x(i) + hk_1/2| - r}{c}\right) \\ &\times \left(1 + \exp\left(\frac{|x(i) + hk_1/2| - r}{c}\right)\right)^{-\alpha-1} + s(i) + n(i), \\ k_3 &= -ab \exp\left(\left|b\left(x(i) + \frac{hk_2}{2}\right)\right|\right) \operatorname{sgn}\left(b\left(x(i) + \frac{hk_2}{2}\right)\right) \\ &+ \frac{v_0}{c} \operatorname{sgn}\left(x(i) + \frac{hk_2}{2}\right) \exp\left(\frac{|x(i) + hk_2/2| - r}{c}\right) \\ &\times \left(1 + \exp\left(\frac{|x(i) + hk_2/2| - r}{c}\right)\right)^{-\alpha-1} \\ &+ s(i+1) + n(i+1), \\ k_4 &= -ab \exp(|b(x(i) + hk_3)|) \operatorname{sgn}(b(x(i) + hk_3)) \\ &+ \frac{v_0}{c} \operatorname{sgn}(x(i) + hk_3) \exp\left(\frac{|x(i) + hk_3| - r}{c}\right) \end{aligned}$$

$$\begin{aligned} & \times \left(1 + \exp\left(\frac{|x(i) + hk_3| - r}{c}\right)\right)^{-\alpha-1} \\ & + s(i+1) + n(i+1), \\ x(i+1) &= x(i) + \frac{h}{6}(k_1 + 2k_2 + 2k_3 + k_4), \end{aligned} \quad (7)$$

where $f(t, x)$ is the right side of the equal sign of Eq. (5) and h is the step size of calculation.

The signal-to-noise ratio gain ($\operatorname{SNR}_{\text{gain}}$) can be used to measure the signal enhancement effect of SR systems. The greater the $\operatorname{SNR}_{\text{gain}}$, the better the signal enhancement effect of the system. The definition is as follows:^[14]

$$\operatorname{SNR}_{\text{gain}} = \operatorname{SNR}_{\text{out}} - \operatorname{SNR}_{\text{in}}, \quad (8)$$

where the positive or negative of $\operatorname{SNR}_{\text{gain}}$ can represent the occurrence or absence of SR. In addition, the larger the value, the better the effect of SR.

2.5. The effects of the system parameters on $\operatorname{SNR}_{\text{gain}}$ of the output signal

In this section, we can evaluate the performance of the SR model from the definition of $\operatorname{SNR}_{\text{gain}}$ and study the $\operatorname{SNR}_{\text{gain}}$ as a function of $\operatorname{SNR}_{\text{in}}$. There are five parameters in the EWSSR system, and the parameters can vary at the same time. Therefore, we use the single variable method to research the influence of different parameters on $\operatorname{SNR}_{\text{gain}}$, so that we can choose a set of relatively optimal systematic parameters. In the experiment, we set the amplitude A of sinusoidal signal to be 0.6 V, the driving frequency $f = 0.01$ Hz, the initial phase 0° , the sampling frequency $f_s = 10$ Hz, and the step size $h = 0.1$. At the same time, in order to ensure the accuracy of the results, the values of $\operatorname{SNR}_{\text{gain}}$ are the averages of the repeated 100 calculations.

Firstly, in order to discuss the influence of parameter a on the system, Fig. 7 shows the $\operatorname{SNR}_{\text{gain}}$ as a function of SNR of the input signal with noise for different a and fixed $b = 1.5$, $c = 0.25$, $v_0 = 5$, $r = 0.8$. It can be seen that the peak value of $\operatorname{SNR}_{\text{gain}}$ increases firstly and then decreases with the increasing a , and the peak gradually shifts to the right. When

$a = 0.25$, the SNR_{gain} is relatively high, so we set $a = 0.25$ for the next study.

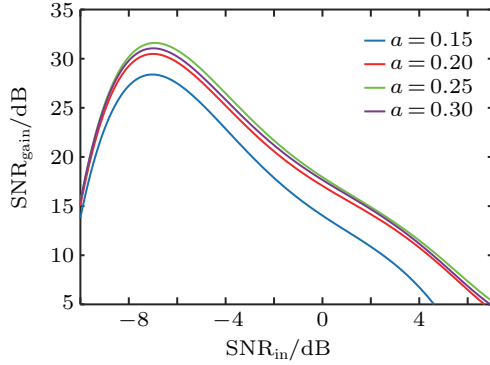


Fig. 7. SNR_{gain} as a function of SNR_{in} with different a and fixed $b = 1.5$, $c = 0.25$, $v_0 = 5$, $r = 0.8$.

Then, we discuss the parameter b . As shown in Fig. 8, it is not difficult to conclude that the detection effect is better in terms of the position of the peak and the value of SNR_{gain} when $b = 2.0$. Therefore, we choose $b = 2$ to continue to study other parameters.

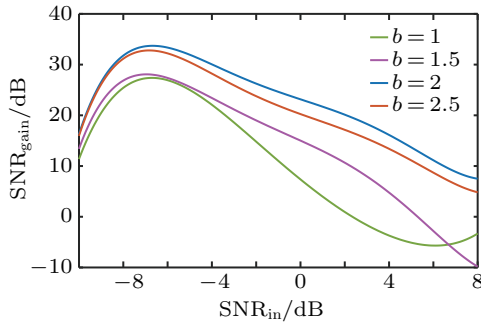


Fig. 8. SNR_{gain} as a function of SNR_{in} with different b and fixed $a = 0.25$, $c = 0.25$, $v_0 = 5$, $r = 0.8$.

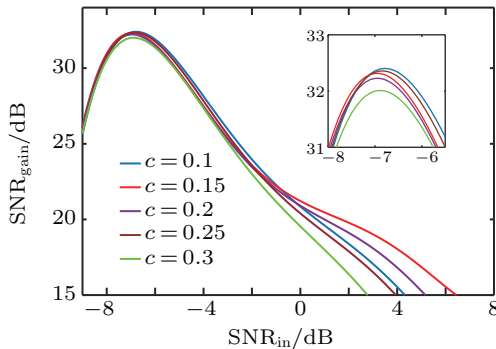


Fig. 9. SNR_{gain} as a function of SNR_{in} with different c and fixed $a = 0.25$, $b = 2$, $v_0 = 5$, $r = 0.8$.

Figure 9 shows the influence of parameter c on the system. Through analysis, it can be seen that under strong noise, it can be seen that when c is changed, the position of the peak is basically unchanged. However, we can determine the relatively suitable c value from a relatively weak noise environment. As seen from Fig. 9, in a relatively weak noise environment, the system has a higher SNR_{gain} when $c = 0.15$. Therefore, we choose $c = 0.15$.

Similarly, figure 10 shows the effect on SNR_{gain} when the system parameter v_0 is changed. By analyzing Fig. 10, under strong noise, the peak of v_0 is higher than other situations when $v_0 = 10$. However, under low noise, the detection effect is almost the same under the conditions of $v_0 = 10$ and $v_0 = 15$. Thus, for comprehensive consideration, we set $v_0 = 10$.

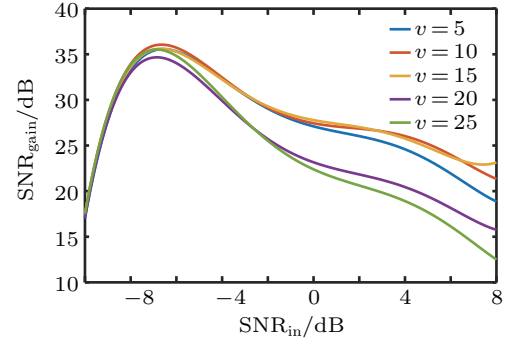


Fig. 10. SNR_{gain} as a function of SNR_{in} with different v_0 and fixed $a = 0.25$, $b = 2$, $c = 0.15$, $r = 0.8$.

Finally, we consider different parameters r . From Fig. 11, we can see that under strong noise condition, $r = 0.2$ is indeed better than other sets of parameters, but there is still a problem that, in the case of weak noise, the detection effect of the system will drop rapidly. Hence, from the overall consideration, we choose $r = 0.4$ as the system parameter. Finally, we identify a set of relatively optimal parameters to establish the system for weak signal detection.

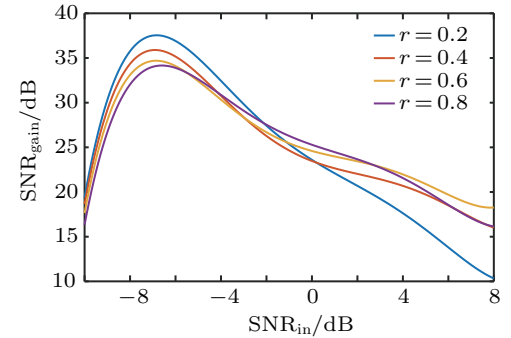
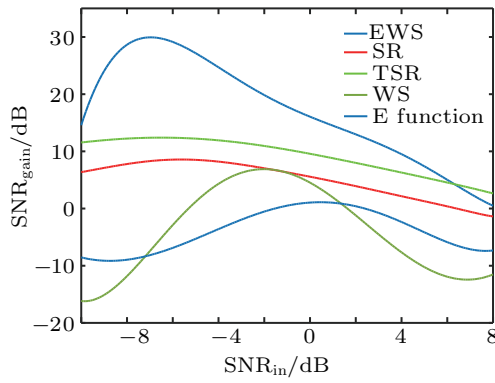


Fig. 11. SNR_{gain} as a function of SNR_{in} with different r and fixed $a = 0.25$, $b = 2$, $c = 0.15$, $v_0 = 10$.

3. Comparison with other SR models

In order to verify the performance of the EWSSR model, we set the previous parameters for simulation experiments, and compare the EWSSR model with other existing SR models, including bistable SR (BSR), tri-stable SR (TSR) and pre-joint models (the WS model and the exponential function (E function)). We set the parameters of SR as $a = 1$ and $b = 1$, the parameters of TSR as $a = 25$, $b = 5$, $c = 0.5$, the parameters of WS as $c = 0.15$, $v_0 = 10$, $r = 0.4$ and the parameters of the E function as $a = 0.25$, $b = 2$. Firstly, we compare SNR_{gain} . The result is shown in Fig. 12.

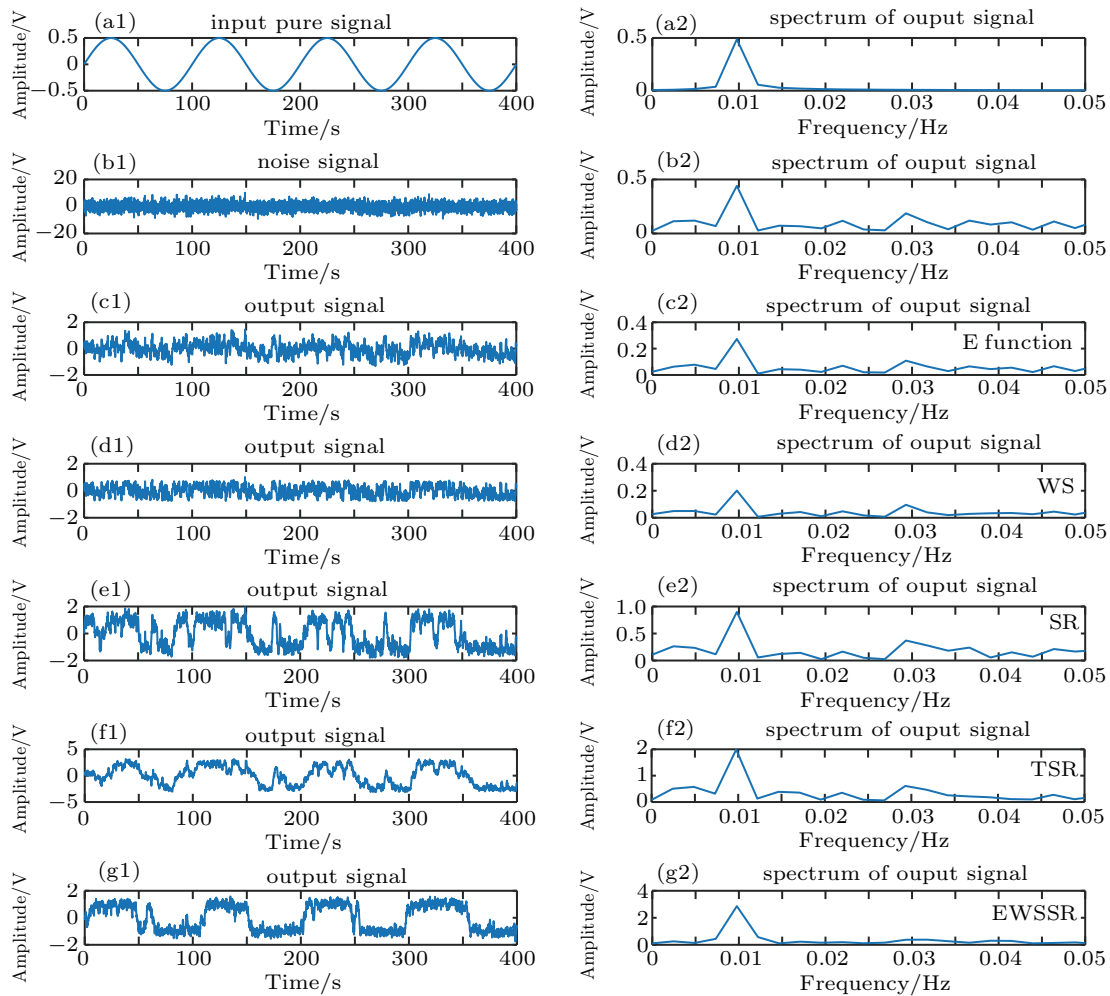

 Fig. 12. Five different systems of SNR_{gain} .

Compared to other SR models, the performance of the EWSSR model is obvious and outstanding. The SNR_{gain} of EWSSR is the highest in almost all ranges of SNR_{in} . This demonstrates that the EWSSR model has not only superior performance of improving the SNR in weak signal detection, especially under strong noise environment, but also better performance in terms of detection range. In other words, the SNR of the EWSSR system can keep high over a wider range. In ad-

dition, we can find that the ranking of performance from high to low in SNR is: EWSSR, TSR, SR, WS, E function.

In terms of SNR, we have verified that the EWSSR model is better than the other four models. In addition, we can also study the detection in time domain and frequency domain to compare the performance of the systems. In order to verify that the EWSSR model not only has better performance under relatively weak noise conditions, but also has good performance under strong noise. We select the different noise intensities D for simulation experiments in both the time domain and frequency domain.

Firstly, we set $D = 2.0$. Figures 13(a) and 13(b) show the original signal without noise and the original signal with Gaussian white noise and their spectra. It can be seen that it is difficult to make a distinction to the original signal in Fig. 13(b). Figures 13(c)–13(g) show that the output signals processed by the E function, WS, SR, TSR, EWSSR and their spectra, respectively. By comparing the peaks in the spectra, it is easy to see that under strong noise conditions, the performance of the EWSSR model is better than the other four models.


 Fig. 13. (a) The original sinusoidal signal and its spectrum. (b) The noise signal and its spectrum. (c)–(g) The output signals with their spectra processed by the E function, WS, SR, TSR, and EWSSR, respectively, for $D = 2.0$.

Then, we set $D = 8.0$. From Fig. 14(b), we can observe that the original signal has been completely submerged by noise. Analyzing Figs. 14(c)–14(f), we find that there are multiple numerically approximate peaks in the spectra so that it will be difficult to determine them if the peak at $F = 0.01$ is

the highest, which can lead to erroneous results. However, the frequency of the signal can still be seen in Fig. 14(g). Therefore, we once again prove the superiority of the EWSSR system. Finally, we prove the advantages of our proposing system from both SNR and the detection in time-frequency domain.

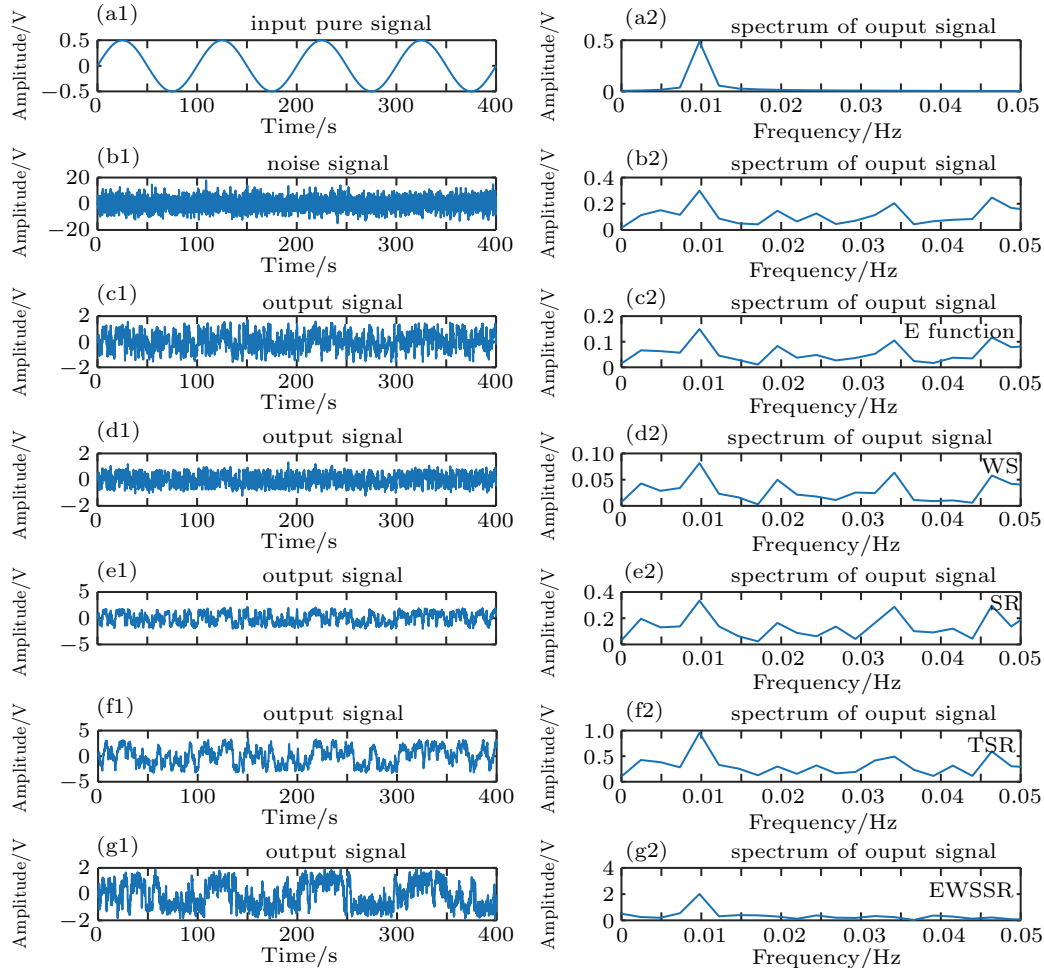


Fig. 14. (a) The original sinusoidal signal and its spectrum. (b) The noise signal and its spectrum. (c)–(g) The output signals with their spectra processed by the E function, WS, SR, TSR, and EWSSR, respectively, when D is equal to 8.0.

4. The experiment of rolling bearing fault signal detection

In this section, we test the EWSSR system, SR system and TSR system using rolling bearing fault signals from the bearing data center of the western reserve universities and compared the three systems. The bearing related information is shown in Table 1. The diameter of the slight peeling fault is 0.007 inches and the depth of the fault is 0.011 inches. CNS bearing center uses accelerometer to collect signals, the sampling time is 4 s, and the sampling frequency is 12000 Hz.

Table 1. Information about 6205–2RS JEM SKF, deep groove ball bearing size/inches.

Inside diameter	Outside diameter	Thickness	Ball diameter	Pitch diameter
0.9843	2.0472	0.5906	0.3126	1.537

The motor speed is 1772 rpm, and the bearing outer ring fault frequency is 3.5848 times the motor rotation frequency.

The motor rotation frequency is $f_g \approx 29.53$ Hz, and the fault frequency is $f_b = 3.5848 \times f_g = 105.871093$ Hz.

When detecting the signal to be tested, the pre-processing is first performed. The envelope spectrum is obtained by Hilbert transform, and then sub-sampling is performed. After the pre-processing is completed, the optimal parameters of the stochastic resonance system are adaptively acquired by the genetic algorithm. Finally, according to the optimal parameters, the stochastic resonance is used to detect the signal to be tested.

Figure 15(a) shows the time domain waveform and frequency domain of the acquired signal. Obviously, the time domain waveform is disorderly, the frequency components in the spectrum are concentrated in 2000–4000 Hz, and f_b of the outer ring of the bearing is not detected.

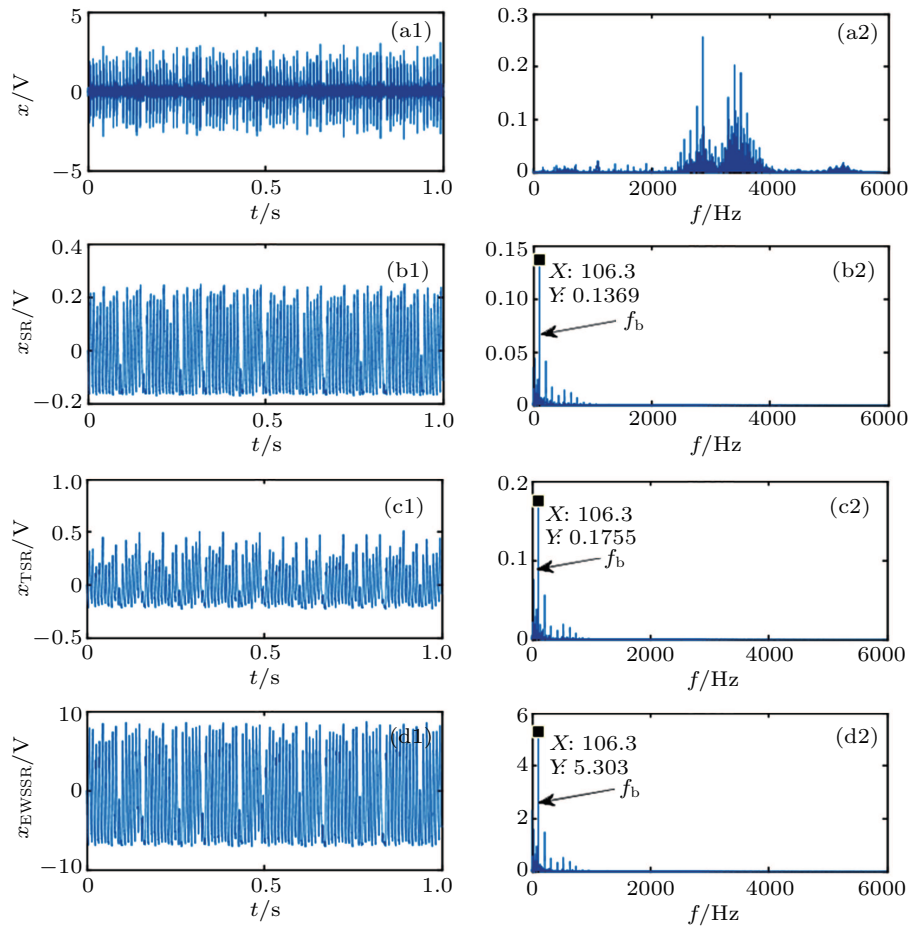


Fig. 15. Processing of bearing outer ring fault signal, time domain diagram and spectrum: (a) input signal, (b) output signal of SR system, (c) output signal of TSR system, and (d) output signal of EWSSR system.

Figures 15(b)–15(d) show that the time domain waveform and spectrum of the output signal processed by the SR system, TSR system and EWSSR system respectively. The frequency at the peak of the spectrum is 106.3 Hz, which is very close to the theoretically calculated fault frequency. Within the allowable range of error, the fault frequency is successfully detected. The optimized stochastic resonance system parameters of SR are $a = 0.02$, $b = 95.42$, $f_{s2} = 49.93$ (f_{s2} is frequency of sub-sampling). The optimized stochastic resonance system parameters of TSR are $a = 34.39$, $b = 42.35$, $c = 1.72$, $f_{s2} = 42.63$. The optimized stochastic resonance system parameters of EWSSR are $a = 0.22$, $b = 0.16$, $v_0 = 3.12$, $c = 2.41$, $r = 4.94$, $f_{s2} = 42.1$. In the spectrum of the output signal of the SR system, the peak value of f_{b2} is 0.1369, and the SNR_{gain} is 28.43 dB. In the spectrum of the output signal of the TSR system, the peak value of f_{b2} is 0.1755, and the SNR_{gain} is 28.52 dB. In the spectrum of the output signal of the EWSSR system, the peak value of f_{b2} is 5.303, and the SNR_{gain} is 29.84 dB. Both the peak value and SNR_{gain} of the EWSSR system are higher than those of the SR and the TSR systems. It can be seen that the proposed EWSSR system can effectively improve the SNR_{gain} in detecting the slight peeling of the outer ring of the rolling bearing.

5. Conclusion

In this paper, a new SR model EWSSR has been proposed. We firstly investigate the influence of system parameters on its characteristics. Then, a set of relatively optimal system parameters are selected based on its performance in the SNR. Moreover, EWSSR and other SR models are compared in terms of SNR and detection effect in time-frequency domain. The experimental results on SNR indicate that the SNR_{gain} of EWSSR is higher than the SR TSR and pre-joint models. The experimental results in the time-frequency domain show that the EWSSR system is better than the other four models in detecting weak signals, especially in the environment of strong noise. Therefore, it is proved theoretically that the proposed model is better at detecting weak signals under strong noise. Finally, we apply the EWSSR model to the detection of actual bearing fault signals. The test results are also superior to the SR and TSR models, which proves the feasibility of this system in actual detection.

References

- [1] Peng H H, Xu X M, Yang B C and Yin L Z 2016 *J. Phys. Soc. Jpn.* **85** 044005
- [2] Luo J J, Xu X M, Ding Y P, Yang B C, Sun K H and Yin L Z 2018 *Eur. Phys. J. Plus* **133** 239

- [3] Li C J, Xu X M, Ding Y P and Yin L Z 2018 *Int. J. Mod. Phys. B* **32** 1850103
- [4] Li M P, Xu X M, Yang B and Ding J F 2015 *Chin. Phys. B* **24** 060504
- [5] Feng J L, Dong J M and Tang X L 2016 *Chin. Phys. Lett.* **33** 108701
- [6] Kong L W, Zheng W R and Fang H P 2016 *Chin. Phys. Lett.* **33** 020501
- [7] Zhang J Q, Huang S F, Pang S T, Wang M S and Gao S 2015 *Chin. Phys. Lett.* **32** 120502
- [8] Liu Y L, Yu X M and Hao Y H 2015 *Chin. Phys. Lett.* **32** 110503
- [9] Song X T, Li H W, Yin Z Q, Liang W Y and Zhang C M 2015 *Chin. Phys. Lett.* **32** 080302
- [10] Benzi R, Sutera A and Vulpiani A 1981 *J. Phys. A: Math. Gen.* **14** L453
- [11] Chapeau-Blondeau F 1997 *Phys. Rev. E* **55** 2016
- [12] Mcnamara B, Wiesenfeld K and Roy R 1988 *Phys. Rev. Lett.* **60** 2626
- [13] Ginzburg Z, Vajtai R and Kiss L B 2000 *Chaos Solitons Fractals* **11** 1929
- [14] Gammaitoni L, Hänggi P and Jung P 1998 *Rev. Mod. Phys.* **70** 223
- [15] Wiesenfeld K and Moss F 1995 *Nature* **373** 33
- [16] Wu J J, Leng Y G and Qiao H S 2018 *Acta Phys. Sin.* **67** 210502 (in Chinese)
- [17] Asdi A S and Tewfik A H 1995 *Acoustics, Speech, and Signal Processing*, May 9–12, 1995, Detroit, MI, USA, p. 1332
- [18] Galdi V, Pierro V and Pinto I M 1998 *Phys. Rev. E* **57** 6470
- [19] Lutz E 2001 *Phys. Rev. E* **64** 051106
- [20] Leng Y G, Leng Y S, Wang T Y and Guo Y 2006 *J. Sound & Vib.* **292** 788
- [21] Jin Y F 2018 *Chin. Phys. B* **27** 050501
- [22] Wang S and Wang F Z 2018 *Acta Phys. Sin.* **16** 160502 (in Chinese)
- [23] Xu W, Wang L, Feng J Q, Qiao Y and Han P 2018 *Chin. Phys. B* **27** 110503
- [24] Zhang X H and Liu S Q 2018 *Chin. Phys. B* **4** 040501
- [25] He Q B and Wang J 2012 *Digital Signal Process.* **22** 614
- [26] Liu J, Li G, Liu S L and Chen Y Q 2004 *Space Med. & Med. Eng.* **17** 360
- [27] Li Q Q, Xu X M, Yin Y Z, Ding Y P, Ding J F and Sun K H 2018 *Chin. Phys. B* **27** 034203
- [28] Wu X J, Guo W M, Cai W S, Shao X G and Pan Z X 2004 *Talanta* **61** 863
- [29] Shi P M, Ding X J and Han D Y 2014 *Measurement* **47** 540
- [30] Lu S L, He Q B and Kong F R 2014 *Mech. Syst. & Signal Process.* **45** 488
- [31] Lu S L, He Q B and Kong F R 2015 *Engineering Asset Management - Systems, Professional Practices and Certification* (Berlin: Springer) pp. 99–108
- [32] Zhang G, Shi J B and Zhang T Q 2018 *J. Electron. Meas. & Instrum.* **32** 142